Proceedings of International Symposium on Bond Behaviour of FRP in Structures (BBFS 2005)
Chen and Teng (eds)

BONDING AND ANCHORING CHARACTERIZATION BETWEEN FRP SHEETS, CONCRETE, AND VISCOELASTIC LAYERS UNDER STATIC AND DYNAMIC LOADING

Xi Huang[1] and Genda Chen[2]

1. Trabue, Hansen and Hinshaw, Inc., Columbia, MO 65202, Email: shuang@thhinc.com
2. Center for Infrastructures Engineering Studies, Department of Civil, Architectural, and Environmental Engineering, University of Missouri-Rolla, 1870 Miner Circle, Rolla, MO 65409-0030, Email: gchen@umr.edu

ABSTRACT

An innovative concept for normalizing the multiple seismic performance objectives of retrofitted structures was recently introduced by the authors. Referred to as a damping-enhanced strengthening, this integrated damping and strengthening strategy included the bonding component between FRP sheets and viscoelastic layers as well as the anchoring component of FRP sheets into concrete. Although anchorage of FRP sheets into concrete with FRP rods was successful in some applications, their joint behaviour under static and dynamic loading needs to be evaluated systematically. This paper presents an experimental research program on the bonding and anchoring characterization among FRP sheets, concrete surface, and viscoelastic layers. The effects of temperature and load rate on the joint properties are investigated. A simple analytical model is proposed based on the ACI design equation.

KEYWORDS

FRP, Anchorage, Bonding, Concrete, Viscoelastic Layer.

INTRODUCTION

Fiber reinforced polymers (FRP) has recently gained more acceptances in civil engineering application due to their superior properties such as high strength, light weight, high resistance to fatigue and corrosion, and especially ease in field installation. Over the past decade, extensive research has been conducted to investigate the behaviour of reinforced concrete (RC) columns strengthened with FRP composites (Matsuda et al. 1990, Priestley and Seible 1991, Saadatmanesh et al. 1994, Seible et al. 1995, Xiao and Ma 1997, Mirmiran and Shahawy 1997, Xiao et al. 1999, Pantelides et al. 1999, Liu et al. 2000). In recent years, the concept of a damping-enhanced strengthening system was proposed to design RC columns for their optimal performance under multi-level earthquake hazards (Chen and Xu 2004). As illustrated in Figure 1, the system consisted of FRP sheets wrapping around a column, viscoelastic (VE) layers outside the FRP wrapping, and another FRP sheet that is used to constrain the motion of the outer surface of the VE layers to the footing. As such, both FRP bonding with VE and FRP anchoring into concrete are critical components of the system.

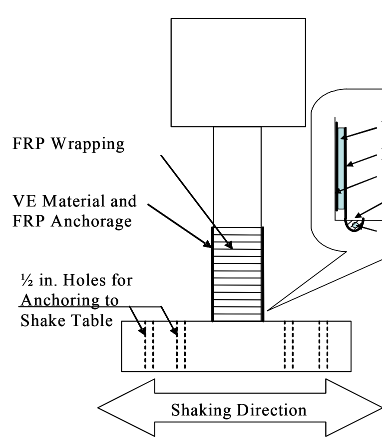

Figure 1. Proposed Retrofit System

Anchoring an FRP sheet into concrete by a FRP rod has been proven to be an effective way to keep the FRP sheet from debonding in the wet lay-up technology of FRP application under slowly-varying loading. It has been successfully used in shear strengthening with FRP sheet U-wraps (Khalifa and Nanni 2000). This paper presents the results from a series of bond and anchorage tests under static and dynamic loading conditions.

SPECIMENS

For bond strength testing, each specimen was designed with carbon FRP sheets and Sorbothane VE/rubber layers. Two VE layers were sandwiched between three FRP sheets, as shown in Figure 2. The middle FRP sheet was made with two plies and the top and bottom sheets were of a single ply of FRP materials. Sorbothane is a thermoset, polyether-based, polyurethane material. It has low creep rate, high damping coefficient, and wide effective temperature range. A total of five types of bond specimens (Types A, B, C, D and E) were tested. Their dimension and hardness are given in Table 1.

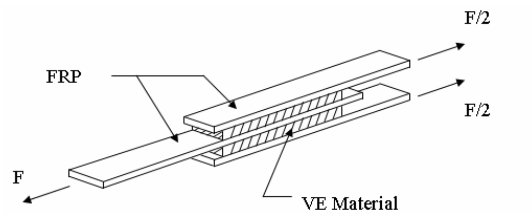

Figure 2. Bonding Test Specimen


Figure 3. FRP Anchorage Specimens

Table 1. Five Types of Bonding Test Specimens

Type	Durometer	One-side Area (in^2)	Thickness (in.)	Volume (in^3)
A	70	3.0	1/8	0.375
B	70	6.0	1/8	0.75
C	70	9.0	1/8	1.125
D	70	6.0	3/16	1.125
E	50	6.0	1/8	0.75

For anchorage testing, each specimen consisted of a 6"×6"×6" concrete block and an FRP sheet that was anchored though a 4" long and 0.5" wide groove into one side of the concrete block by varying depths (0.5", 1.0", and 1.5"). The FRP anchorage was constructed in three steps. First, MBrace Saturant resin, the same epoxy as used for bonding FRP and VE material, was poured to fill half of the groove. A 2" wide FRP sheet was then pushed into the groove with a 4" long #3 FRP rod. Finally, additional MBrace Saturant resin was poured on top of the FRP rod to fill up the groove. One-day cured FRP anchorage specimens are shown in Figure 3.

TEST PROGRAM, FACILITY, AND INSTRUMENTATION

Static bond tests were conducted with one of each of the five specimens in Table 1 by applying displacement at a rate of 0.1 in/min. After the ultimate shear strength and strain have been determined, dynamic bond tests were carried out on eight Type B specimens, designated as D1 to D8 in Table 2. Each specimen was tested to failure under a series of harmonic loads of incrementally-increasing amplitude as illustrated in Figure 4. Each harmonic load repeated for ten cycles at constant excitation period (T), amplitude increment (a), and average load (F_0). The tension load (F_0) was introduced to prevent potential buckling of the test specimens under dynamic loading.

Table 2. Dynamic Bonding Test Matrix

Specimen Type	Initial Temperature (°F)	Initial Strain (in./in.)	Initial Stress (psi)	Frequency (Hz)
D1	0	1.0	20	2.0
D2	0	1.5	30	2.0
D3	75	2.0	40	0.1
D4	75	2.0	40	2.0
D5	75	1.5	30	2.0
D6	75	1.5	30	4.0
D7	120	1.5	30	2.0
D8	120	2.0	40	2.0

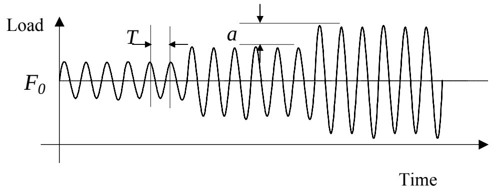

Figure 4. Dynamic Bond Test Loading

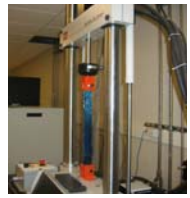
Figure 5. Bond Test Setup


Figure 6 Infrared Thermometer

Each bond specimen was tested in a displacement-controlled mode on the MTS 858 testing machine with a stroke capacity of 4.5″ and an axial hydraulic force of 5.5 kips in both compression and tension. The testing machine MTS 858 and test setup is shown in Figure 5. Both load and displacement were recorded during each test with an internal load cell and an internal LVDT of the test's machine. The temperature at the surface of each specimen was measured with an infrared thermometer, as shown in Figure 6.

A dozen anchorage specimens were tested as indicated in their test matrix in Table 3. In addition to the groove depth, loading rate was considered as another test parameter in this series of tests, as shown in Table 3. Testing of FRP anchorage specimens was conducted on the MTS 880 machine equipped with a digital data acquisition system interfaced with LabView. Since it is difficult, if not impossible, to fix a concrete block directly on the MTS 880 machine, a steel cage frame was used in each test as part of the test apparatus. The setup of an anchorage test is schematically shown in Figure 7. A concrete block was set on the bottom plate of the steel cage. FRP sheet anchored into the concrete block went through a gap on the bottom steel plate and fixed with the loading head clamps of the MTS 880 machine. While FRP sheet is subjected to a tension load, a reacting compression force will be developed on the bottom face of the concrete block. To reduce this effect, two 0.75″ thick steel plates were placed 4″ apart between the concrete block and the bottom plate of the steel cage. The load applied to each specimen was recorded with an internal load cell and the displacement between two ends of each specimen was measured with an external LVDT.

Table 3. Test Matrix of FRP Anchorage Test under Static Loading

Specimen	Groove Depth (in.)	Loading Rate (in./min)
AS1	1.0	0.007
AS2	1.0	0.025
AS3	1.0	0.025
AS4	1.0	0.025
AS5	1.0	0.100
AS6	1.0	0.300
AS7	0.5	0.025
AS8	0.5	0.025
AS9	0.5	0.025
AS10	1.5	0.025
AS11	1.5	0.025
AS12	1.5	0.025

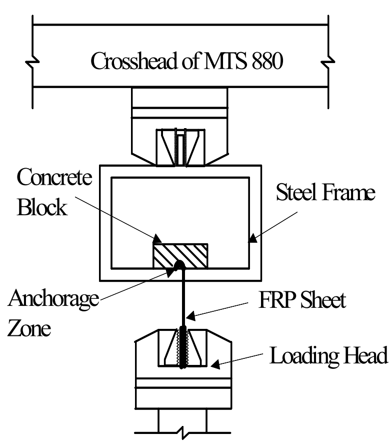

Figure 7. Set-up of Anchorage Test

TEST RESULTS AND DISCUSSIONS

The mechanical properties of FRP sheets and Sorbothane are summarized in Tables 4 and 5, respectively, based on the technical data provided by manufacturers.

Table 4. Material Property of FRP Sheets

Fiber Type	Thickness (in.)	Design Strength (ksi)	Design Strain (in./in.)	Tensile Modulus (ksi)
Carbon	0.0065	550	0.017	33000

Table 5. Material Property of VE Layers

Durometer	Tensile Strength (psi.)	Elongation at Break (%)	Young's Modulus at 5 Hz (psi)	Temp. Range (°F)
70	206	399	120	-20~160

Bonding tests were conducted under both static and dynamic loading. It was observed that all specimens failed in tearing of the VE layers, as illustrated in Figure 8, indicating that the bonding strength between a CFRP sheet and a VE layer with Mbrace saturant resins was sufficiently strong. Under static loading, the shear stress and strain curves of five Type B bond specimens are presented in Figure 9 at five different temperatures. These curves consistently indicate the linearity between stress and strain at small strains. As strain further increases, the stress-strain curve becomes concave upward due mainly to the reduced thickness of a VE layer so that the shear stiffness of the VE layer is increased. At low temperature, the VE material exhibits relatively higher ultimate strength and ultimate shear strain. The stiffness of the VE material also decreases as temperature increases. All these can be explained by the softening effect of VE materials under high temperature. The ultimate strains of the tested specimens are all over 350% in the temperature range from 0°F to 120°F. This indicates that the value (399%) suggested by manufacturer is only slightly over estimated at high temperature. For this reason, a design ultimate strain of 300% is recommended.

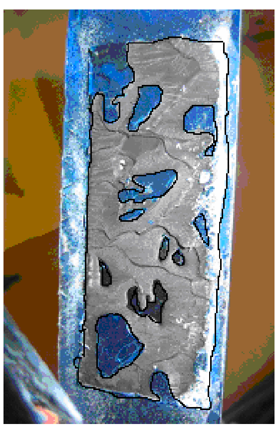

Figure 8. Failure Mode

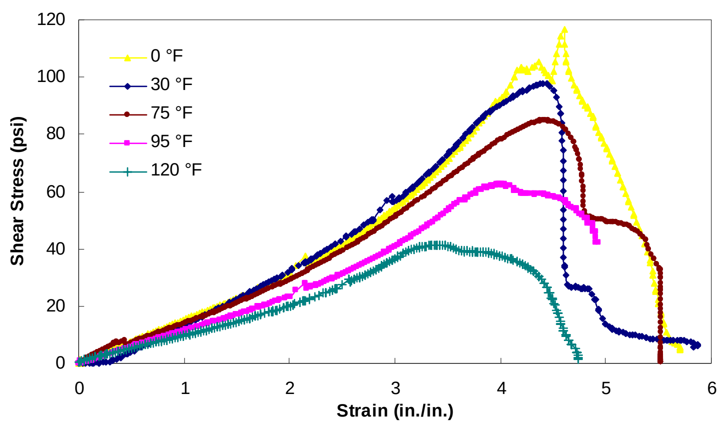

Figure 9. Stress-strain Curves of Bond Specimens under Static Loading

Dynamic bond tests were conducted at room temperature. The test results are summarized in Table 6. Specimens D1, D4, D5 and D8 did not fail during dynamic tests. This means that each of these specimens can withstand such cyclic displacements without failure. Specimens D2, D3 and D7 failed in the same mode (tearing VE material) as observed during static bond tests. During dynamic testing, stress relaxation of VE materials was observed especially for Specimen D3 that was tested for approximately 27 minutes at a frequency of 0.1 Hz.

In comparison with Figure 9, Table 6 indicated that bonding performance of the specimens under dynamic loading is quite different. In general, the bonding strength increased while the strain range at failure was reduced under dynamic loading, especially for those specimens tested under a higher initial loading. However, all the specimens were able to withstand a maximum strain of over 300% before VE layers were torn apart or at the end of each testing. Indeed, for the damaged specimens, the minimum VE strain was 314%. Considering that Specimen D8 failed after 50 cycles of loading, the recommended strain of 300% for the design of VE layers from static bonding tests is acceptable under dynamic loading.

Table 6. Dynamic Bonding Test Results

Specimen	Maximum Stress (psi)	Strain Range in Last Cycle	Temperature after Test (°F)	Specimen Condition
D1	92	-1.00~3.00	20	Undamaged
D2	122	-0.50~3.50	18	Damaged
D3	121	0.64~3.43	82	Damaged
D4	122	0.00~4.00	80	Undamaged
D5	92	-0.50~3.50	83	Undamaged
D6*	75	0.00~3.00	82	Undamaged
D7	68	-0.50~3.50	123	Undamaged
D8	73	0.89~3.14	124	Damaged

*: Test incomplete.

The load-displacement curves of the anchorage specimens with a 1″ deep groove are shown in Figure 10. They are slightly different from expected of straight lines up to failure. The curved parts in the early stage of tests are attributable to the imperfect contact between the concrete block and the steel plates, which results from either a rough concrete surface or small debris particles between the concrete and the steel plates. During testing, those small particles or bumped-out concrete will be crashed due to stress concentration, leading to reduction in the load at a given displacement. After an even contact surface is formed, the interfacial force is distributed evenly on the contact area and increases proportionally with the displacement the test specimen experiences.

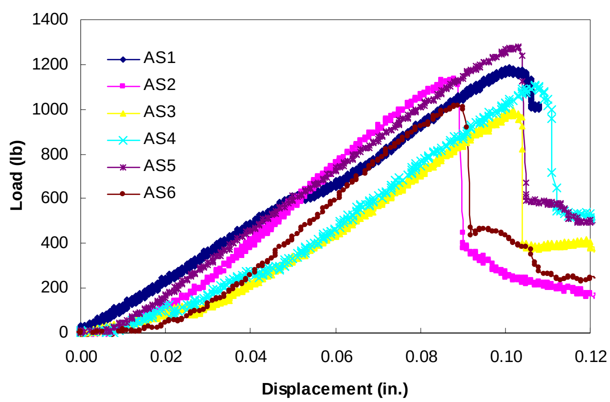

Figure 10. Load-displacement Curves of FRP Anchorages

All anchorage specimens were observed to fail due to rupture of the concrete, as indicated by sudden drop in the load-displacement curves, Figure 10. Concrete strength is thus a controlling factor for the FRP anchorage. A typical failure mode of the specimens is shown in Figure 11. It is seen from Figure 11 that the crack in concrete starts somewhere away from the side of a steel plate. This indicates that the potential impact of the steel plates on the formation of a failure mechanism is no longer a major concern.

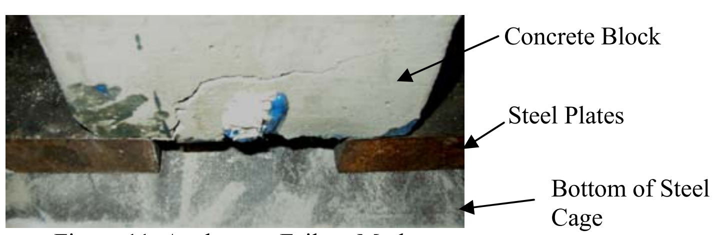

Figure 11. Anchorage Failure Mode

Based on the static test results and failure mechanisms from all 12 specimens shown in Table 4, a design equation for the anchorage strength is proposed as follows:

$$V_c = 4\sqrt{f_c^{'}}\, l_R d_G \qquad (1)$$

in which f'_c is the compressive strength of concrete, d_G and l_R represents the vertical area counted for shear resistance, d_G is the depth of the groove, and l_R is the length of the FRP rod. To validate Equation (1), the predicted shear strengths of the specimens were compared in Table 7 with the average experimental results in Table 6 for each groove depth. Clearly, the predicted results are in good agreement with the experimental data.

Table 7. Predicted versus Average Experimental Shear Strength of FRP Anchorages

Groove Depth (in.)	Experimental (lb)	Predicted (lb)	Difference (%)
0.5	572	527	8
1.0	1107	1054	5
1.5	1519	1582	-4

CONCLUSIONS

Based on the test results, the following conclusions can be drawn:

- The bonding mechanism between VE layers and FRP sheets with Mbrace saturant epoxy was found very effective. It failed by tearing the VE layers apart. The bond strength was therefore controlled by the ultimate strain of VE materials. A design shear strain of 300% is recommended for the proposed retrofitting system.
- The strength of a mechanical bond between FRP sheets and VE layers increases under dynamic loading while the strain range at failure decreases. However, all the specimens tested were able to withstand a maximum strain of over 300% before VE layers were torn apart or at the end of each testing. Therefore, the recommended strain of 300% for the design of VE layers from static bonding tests is acceptable under dynamic loading.
- The anchorage mechanism of FRP sheets into concrete by a FRP rod can effectively transfer damping forces from column through VE layers and FRP anchoring sheets to column footing. The potential failure mode of the anchorage is concrete rupture. For a given depth, the strength of the anchorage depends on the concrete strength due to the high strength of FRP sheets.
- A simple design equation was developed based on the shear rupture of concrete along two surfaces between FRP and concrete. The equation proposed for the design of anchorages can predict the anchorage strength that agrees very well with experimental results.

REFERENCES

Chen, G. and B. Xu. (2004). “Challenges and Opportunities in Performance-Bsed Design of Seismic Structures.” Proc., Int. Conf. on Earthquake Engrg., Nanjing, China.

Khalifa, A. and Nanni, A. (2000). “Improving Shear Capacity of Existing RC T-Section Beams Using CFRP Composites.” Cement and Concrete Composites, 22(2), 165-174.

Liu, H., Tai, N., and Chen, C. (2000). “Compression strength of concrete columns reinforced by non-adhesive filament wound hybrid composites.” Composites - Part A: Applied Science and Manufacturing, 31(3), 221-233.

Matsuda, T., Sato, H., Fujiwara, H., and Higashira, N. (1990). “Effect of carbon fiber reinforcement as a strengthening measure for reinforced concrete bridge piers.” Proc., 1st U.S.-Japan Workshop on Seismic Retrofit of Bridges.

Mirmiran, A., and Shahawy, M. (1997). “Behavior of concrete columns confined by fiber composites.” J. Struct. Eng., 123(5), 583–590.

Pantelides, C.P., Gergely, J., Reaveley, L. D., and Volnyy, V. A. (1999). “Retrofit of RC bridge pier with CFRP advanced composites.” J. Struct. Eng., 125(10), 1094-1099.

Priestley, M. J. N., and Seible, F. (1991). “Seismic assessment and retrofit of bridges.” Struct. Sys. Res. Proj., Rep. No. SSRP-91/103, University of California at San Diego, CA.

Saadatmanesh, H., Ehsani, M. R., and Li, M. W. (1994). “Strength and ductility of concrete columns externally reinforced with fiber composite straps.” ACI Struct. J., 434.

Seible, F., Hegemier, G. A., and Innamorato, D. (1995). “Developments in bridge column jacketing using advance composites.” Proc., Nat. Seismic Conf. on Bridges and Hwy., Federal Highway Administration and California Department of Transportation.

Xiao, Y., and Ma, R. (1997). “Seismic retrofit of RC circular columns using prefabricated composite jacketing.” J. Struct. Eng., 123(10), 1357-1364.

Xiao, Y., Wu, H., and Martin, G. R. (1999). “Prefabricated composite jacketing of RC columns for enhanced shear strength.” J. Struct. Eng., 125(3), 255-264.